Received: 1 September 2023 | Revised: 28 November 2023 | Accepted: 4 January 2024

DOI: 10.1002/glr2.12071

Grassland Research

RESEARCH ARTICLE

Integrated transcriptome and proteome analyses reveal potential mechanisms in *Stipa breviflora* underlying adaptation to grazing

Yanan Liu[1] | **Shixian Sun**[2] | **Yanan Zhang**[1] | **Miaomiao Song**[1] | **Yunyun Tian**[3] | **Peter J. Lockhart**[4] | **Xin Zhang**[1] | **Ying Xu**[1] | **Zhenhua Dang**[1]

[1]Ministry of Education Key Laboratory of Ecology and Resource Use of the Mongolian Plateau & Inner Mongolia Key Laboratory of Grassland Ecology, School of Ecology and Environment, Inner Mongolia University, Hohhot, China

[2]Institute of Grassland Research, Chinese Academy of Agricultural Sciences, Hohhot, China

[3]Ministry of Education Key Laboratory of Herbage & Endemic Crop Biotechnology, School of Life Sciences, Inner Mongolia University, Hohhot, China

[4]School of Natural Sciences, College of Sciences, Massey University, Palmerston North, New Zealand

Correspondence

Zhenhua Dang, Ministry of Education Key Laboratory of Ecology and Resource Use of the Mongolian Plateau & Inner Mongolia Key Laboratory of Grassland Ecology, School of Ecology and Environment, Inner Mongolia University, Hohhot 010021, China.
Email: zhdang@imu.edu.cn

Handling Editor: Cory Matthew

Funding information

National Natural Science Foundation of China, Grant/Award Number: 32160088; Program for Young Talents of Science and Technology in Universities of Inner Mongolia Autonomous Region of China, Grant/Award Number: NJYT22093; Open Project Program of Ministry of Education Key Laboratory of Ecology and Resources Use of the Mongolian Plateau

Abstract

Background: Long-term overgrazing has led to severe degradation of grasslands, posing a significant threat to the sustainable use of grassland resources.

Methods: Based on the investigation of changes in functional traits and photosynthetic physiology of *Stipa breviflora* under no grazing, moderate grazing, and heavy grazing treatments, the changes in expression patterns of genes and proteins associated with different grazing intensities were assessed through integrative transcriptomic and proteomic analyses.

Results: Differentially expressed genes and proteins were identified under different grazing intensities. They were mainly related to RNA processing, carbon metabolism, and secondary metabolite biosynthesis. These findings suggest that long-term grazing leads to molecular phenotypic plasticity, affecting various biological processes and metabolic pathways in *S. breviflora*. Correlation analysis revealed low correlation between the transcriptome and the proteome, indicating a large-scale regulation of gene expression at the posttranscriptional and translational levels during the response of *S. breviflora* to grazing. The expression profiles of key genes and proteins involved in photosynthesis and phenylpropanoid metabolism pathways suggested their synergistic response to grazing in *S. breviflora*.

Conclusions: Our study provides insight into the adaptation mechanisms of *S. breviflora* to grazing and provides a scientific basis for the development of more efficient grassland protection and utilization practices.

KEYWORDS

functional traits, grazing adaptation, photosynthetic physiology, proteome, *Stipa breviflora*, transcriptome

INTRODUCTION

Grasslands are an important natural resource in terrestrial ecosystems. Inner Mongolian grassland is part of the Eurasian grasslands, accounting for 22% of China's grassland area (Yu et al., 2020). It is an important ecological biome providing ecological security and ecosystem services and stability in northwest China. However, because of long-term overgrazing and irrational utilization of grasslands and impacts of climate change in recent decades, the Inner Mongolian grassland has been seriously degraded. This has impacted negatively on the ecology of the regional landscape and is a great threat to the sustainable development of grasslands in pastoral areas (Cui et al., 2012; Liu et al., 2017). Grazing is an important means of utilization of grassland resources and the main driver of changes in plant traits in grasslands (Zhao et al., 2016). Under natural conditions, plants adapt to external environmental stresses by changing their functional traits such as height, clump width, stem and leaf

Yanan Liu and Shixian Sun contributed equally to this study.

mass, and dry matter content (Li et al., 2014). Previous studies investigating the effects of grazing on grassland ecosystems have mostly been conducted at the macro level, such as landscape patterns and plant community composition. In addition, the functional traits of plants have been studied. Many such studies have focused on the development and evolution of these traits and their relationship with the environmental changes and stresses. These studies are relevant for further investigating the mechanisms underlying the response of forage grasses to grazing and grassland productivity formation and productivity decay under grazing. Studies have suggested that the response of steppe plants to grazing is mainly reflected in the growth pattern of plants, with the most obvious indicators being stems and leaves of whole plants (Liu et al., 2019; Orwin et al., 2018; Wang et al., 2021). In a typical grassland under grazing in Inner Mongolia, plant height and biomass in *Agropyron cristatum* were the factors that were altered to the highest degree, whereas leaf number (LN), length, and width hardly changed (Li et al., 2021). Moreover, functional traits have been observed to vary between years with abundant water and drought. In a study, the most significantly affected functional traits of *Leymus chinensis* (a C3 plant species) and *Cleistogenes squarrosa* (a C4 plant species) were found to be the stem and leaf traits (Zheng et al., 2010). The researchers explored the morphological characteristics of *C. squarrosa* in typical grassland communities under grazing disturbance, and found significant changes in plant height, stem-to-leaf ratio, and LN (Xing et al., 2019). Such responses in morphological characteristics of plants are considered important indicators for predicting impacts of environmental and climate changes (Lienin & Kleyer, 2012).

Steppe plants have gradually developed adaptive defense strategies in response to grazing by herbivores. Their defense strategies can be classified as grazing avoidance and/or grazing tolerance (Rotundo & Aguiar, 2007). An example of a grazing avoidance strategy is synthesis of secondary metabolites such as tannins, terpenoids, and betaine by plants to deter consumption by livestock (Lisonbee et al., 2009; Rotundo & Aguiar, 2007; Srinivasa, 2018). Other examples include the presence of awns in grasses such as *Stipa grandis* and *S. breviflora* and the presence of vascular bundles in the leaves of *C. squarrosa*, which reduce the palatability of plant tissue. Grazing tolerance occurs when plants modify their metabolism to aid their survival when being grazed. This may include changes to physiological and biochemical characteristics of plants such as redistribution of carbohydrates and increased photosynthetic rate, cell membrane osmoregulatory capacity, and phytohormone secretion (Benot et al., 2019; Dang et al., 2021; Zhao et al., 2021). A study assessed the physiological indicators of desert grassland forage plants in response to grazing. In this study, free proline, soluble sugar contents, and the activities of superoxide dismutase, peroxidase, catalase, and other protective enzymes all increased in terms of their levels of activity in forage leaves (Ma, 2008). Under grazing conditions, a significant secondary correlation was also observed between the stock carrying rate in grassland and the concentration of endogenous hormones in *S. breviflora* (Jia et al., 2019).

In recent years, exploration of the response mechanism of grassland plants to grazing at the cellular level has garnered much interest. Under simulated grazing conditions, alterations in gene expression related to signal transduction, microRNA regulation, cell wall modification, metabolism, hormone synthesis, and molecular transport proteins were identified in *Oryza sativa*, providing insights into the molecular mechanisms of the response of plants to grazing (Chen et al., 2009). In *Medicago sativa*, hexokinase expression increased after grazing, suggesting that it may play an important role in grazing tolerance in alfalfa (Wang et al., 2016). Via transcriptome sequencing, endogenous genes associated with trauma, drought, and defense in *S. grandis* in response to grazing have been investigated (Wan et al., 2015). Under the stress of overgrazing, in *Poa annua* growing on the Mongolia Plateau, regulation of genes associated with photosynthesis, oxidative phosphorylation, proteases, peroxidases, fatty acid degradation, and the Notch signaling pathway was observed to adapt to grazing stress. Though these results are insightful, the grazing response strategies of different steppe plants need to be studied in detail. Furthermore, understanding of the stress responses of more steppe plants is necessary to develop appropriate measures for grassland resource management and efficient utilization and restoration of damaged grasslands.

S. breviflora is a dominant species in the Inner Mongolian desert grassland. It plays a key role in protecting grassland ecosystems and maintaining grassland–pastoral systems. In this study, we have investigated the responses in *S. breviflora* under long-term grazing conditions by phenotypically observing the alterations in morphological and photosynthetic characteristics. Subsequently, we investigated the expression profiles of genes and proteins of *S. breviflora* in response to various grazing intensities and identified the associated cellular processes and metabolic pathways triggered by grazing and explored nonsynergistic expression patterns between the transcriptome and the proteome. Moreover, we identified and discussed the key differentially expressed genes (DEGs) and/or differentially expressed proteins (DEPs) related to the response and adaptation to grazing in *S. breviflora*.

MATERIALS AND METHODS

Study site and grazing intensities

The grazing experiment was performed at Zhu Rihe Town, Ulanchap, Inner Mongolia, China (112°47′16.9″ E, 42°16′26.2″ N), at an altitude of 1100–1150 m. The average annual precipitation in this area is 183 mm, and the average annual temperature is 5.8°C, which is a mesothermal climate. The soil in this area is a zonally distributed light chestnut calcium soil, which is found in transitional zones from desert grassland to desert. The grazing experiment was started in 2010, with grazing

starting in May and ending at the end of October each year. During this grazing period, the grassland was continuously grazed, and sheep continued grazing at night and did not receive supplementary feeding. The area of each experimental plot was 2.60 hm^2. *S. breviflora* was sampled during grazing from May to October: no grazing (NG; no sheep), moderate grazing (MG; 1.92 sheep ha^{-1}), and heavy grazing (HG; 3.08 sheep ha^{-1}).

Plant material collection

S. breviflora samples were collected from 09:00 a.m. to 11:00 a.m. on a sunny day on August 9, 2020. In total, 10 healthy, mature, and similarly spaced clumps of *S. breviflora* were randomly selected from each of the three plots with various grazing treatments. The young leaves were collected, immediately frozen in liquid nitrogen, and stored at −80°C for subsequent transcriptomic sequencing and quantitative protein isobaric tagging (IBT) analysis. Three biological replicates were set up for each grazing treatment.

Assessment of functional traits and photosynthetic physiology

Photosynthetic physiological indicators including net photosynthetic rate (P_n), stomatal conductance (G_s), transpiration rate (E), and intercellular CO_2 concentration (C_i) were measured using a LI-6400 portable photosynthesis system (Li-COR; Lincoln). In each grazing intensity sample, 10 randomly selected *S. breviflora* plants were investigated. Field measurements were conducted for vegetative tiller height (VH, cm), reproductive tiller height (RH, cm), central height (CH, cm), LN (count), and clump width (CW, cm^2). Subsequently, the above samples were harvested and transported to the laboratory. The leaf area (LA, cm^2) was measured using an EPSON Scan scanner, while the leaf saturated fresh weight (LSFW, g) was determined 24 h after immersion in water. The clusters were then placed in a constant drying incubator at 65°C to measure stem dry weight (SDW, g) and leaf dry weight (LDW, g).

All functional trait and photosynthetic physiological indexes were statistically analyzed using Excel 2019 and SPSS19.0 (SPSS Inc.) software, respectively. The significance of differences in each functional trait and photosynthetic physiological index between grazing treatments was assessed using one-way analysis of variance based on the least significant difference method at $p < 0.05$. Data were expressed as mean ± standard error and plotted using Origin 9.0 (Origin Lab).

RNA extraction and cDNA library construction

Total RNA was extracted from each sample using Trizol reagent (Invitrogen) according to the manufacturer's instructions. The integrity of the RNA was checked using an Agilent2100 Bioanalyzer (Agilent Technologies). The messenger RNA (mRNA) was isolated using Oligo (dT) beads and used as templates to obtain complementary DNA (cDNA) after reverse transcription. Fragment ends were repaired and subjected to polymerase chain reaction, followed by poly (A) ligation and fragment length selection to construct cDNA libraries. Finally, the cDNA library for each sample was paired-end sequenced using the BGISEQ-500 platform by BGI Tech Solution Co., Ltd.

RNA-seq data filtering and bioinformatic analysis

The raw sequence reads from all samples were filtered using Trimmomatic (version 0.36) (Bolger et al., 2014). The process involved removal of reads contaminated with adapters, low-quality reads (>20% low-quality nucleotides), and reads containing ambiguous nucleotides (>5% N). The resulting clean reads were counted using SOAPnuke (version 1.4.0) (Chen et al., 2018). For transcriptome assembly, the clean reads from each sample were de novo assembled using Trinity (version 2.0.6) (Grabherr et al., 2011) with an optimized k-mer length of 25. Subsequently, TGICL (version 2.1) (Pertea et al., 2003) was used for clustering and redundancy elimination, resulting in a collection of unigenes. The unigenes obtained from all samples were further clustered using TGICL to generate nonredundant and nonextendable assemblies, which are referred to as all-unigenes. To assess the completeness of the assembled transcriptomes, a Benchmarking Universal Single-Copy Orthologs (BUSCO) analysis was conducted using 303 conserved sequences from the eukaryotic database (Simão et al., 2015).

The clean reads of each sample were mapped to the merged transcriptome using Bowtie2 (version 2.2.5) (Langmead & Salzberg, 2012), and the mapped reads of each sample were quantified using RSEM (version 1.2.8) (Li & Dewey, 2011) based on the comparison results using transcripts per kilobase per million mapped reads (TPM) to normalize the expression level of genes. Functional annotation was performed by using BLASTX to compare the transcripts with the sequences in the public database, and the significance threshold E value was set to $\leq 10^{-5}$. The databases used were NCBI nonredundant protein (NR), Swiss prot, Clusters of Orthologous Groups, and Kyoto Encyclopedia of Genes and Genomes (KEGG). According to the NR annotations, Blast2GO (version 2.5.0) (Conesa et al., 2005) was used to annotate the Gene ontology (GO) function of all transcripts. DESeq. 2 was used to identify the DEGs between two grazing treatments with the threshold of $|\log_2(\text{fold change})| \geq 1$ and a false discovery rate (FDR) ≤ 0.05. Further, the DEGs under each comparison were subjected to GO and KEGG enrichment analyses using MapMan (version 3.6.0) (Thimm et al., 2004).

Protein preparation

To an appropriate amount of *S. breviflora* leaves, 5% polyvinyl polypyrrolidone powder and a suitable volume of homogenate buffer were added. The mixture was crushed and ground in a grinder. Twice the volume of

Tris-saturated phenol was added; the mixture was vigorously shaken and centrifuged. The upper phenol phase was collected; five times the volume of 0.1 mol L^{-1} cold ammonium acetate/methanol and dithiothreitol (DTT) at a final concentration of 10 mmol L^{-1} were added to this and centrifuged. These steps were repeated twice. To this, 1 mL of cold acetone was added. The mixture was incubated at −20°C for 30 min and centrifuged for 15 min. The supernatant was discarded. The precipitate was air-dried, and an appropriate amount of 1× cocktail with sodium dodecyl sulfate (SDSL3) and EDTA at the final concentration were added. The mixture was thoroughly mixed and incubated on ice for 5 min, followed by the addition of DTT at a final concentration of 10 mmol L^{-1}. The mixture was further ground using a grinding instrument (60 Hz, 2 min) and centrifuged at 25 000*g* for 15 min. The supernatant was discarded, and DTT at a final concentration of 10 mmol L^{-1} was added to this. The mixture was incubated in a water bath at 56°C for 1 h. Iodoacetamide was added at a final concentration of 55 mmol L^{-1}, followed by incubation in the dark for 45 min. To this, 1 mL of cold acetone was added, incubated at −20°C for 2 h, and centrifuged at 25 000*g* for 15 min. The supernatant was discarded, and the precipitate was air-dried. An appropriate amount of SDSL3-free solution was added to this, and the mixture was ground using a grinder (60 Hz, 2 min). The mixture was centrifuged at 25 000*g* for 15 min. The resulting supernatant, containing proteins, was stored at −80°C till further analysis.

Liquid chromatography with tandem mass spectrometry analysis

Each fraction was resuspended in loading buffer (5 mmol L^{-1} ammonium formate containing 2% acetonitrile [ACN]; pH 10) and separated using high hydrogen reverse-phase liquid chromatography (RPLC) on an Ultra Performance LC system (Waters). Solvents A and B consisted of 2% ACN (pH 10, adjusted with ammonia) and 80% ACN (pH 10, adjusted with ammonia), respectively. Gradient elution was performed on a high-pH RPLC column (C18, 1.7 μm, 2.1 mm × 150 mm; Waters), starting with 0 B solvent and increasing to 30% solvent B over 2–38 min, followed by a gradient from 30% to 100% solvent B from 38 to 40 min.

Protein quantification and bioinformatic analysis

The quantitative analysis of IBT was performed using BGI's IQuant software (Wen et al., 2014), applying a 1% FDR filter at the spectrum peptide level (FDR ≤ 0.01). Subsequently, using the parsimony principle, peptides were assembled into proteins, generating a set of protein sequences. At the protein level, another round of filtering was conducted with a 1% FDR threshold to control the false positivity rate. The coefficient of variation (*CV*) value was used to assess quantitative repeatability. Significant DEPs were identified using the criteria of |fold change| ≥ 1.5 and $p \leq 0.05$. Functional annotations using GO, KEGG, and KOG enrichment analyses and subcellular localization analysis of DEPs were conducted.

Correlation analysis between transcriptome and proteome data

The transcriptome and proteome of *S. breviflora* under NG, MG, and HG treatments were compared and correlated. When a protein was expressed at the transcriptome level, the transcriptome and proteome were considered to be correlated. According to the level of change in the protein and transcript levels, the proteins were divided into nine quadrants, and subsequently, enrichment analyses were performed.

Parallel reaction monitoring (PRM) validation

In August 2022, leaf samples of *S. breviflora* were collected from the same grazing plots as those used for transcriptome and proteome sequencing. The proteins from the leaves were sequentially extracted, digested, and separated using high-performance liquid chromatography. Further, the target proteins were analyzed by PRM mass spectrometry using the Q-Exactive HF mass spectrometer (Thermo Scientific). The raw PRM files were processed using Skyline software (MacLean et al., 2010).

RESULTS

Functional traits of *S. breviflora* under various grazing intensities

S. breviflora showed significant differences in landscape characteristics under different grazing intensities. Specifically, with increase in grazing intensity, the surface exposure area increased, the canopy height of plant communities decreased, and the aboveground biomass (including litter) decreased (Figure 1).

The functional traits of *S. breviflora* under different grazing intensities were investigated. The phenotype of whole plants varied under various intensities and showed a tendency of restrained growth as the grazing intensity increased. Among the investigated traits, RH, LDW, LSFW, LA, and CW significantly differed under different grazing treatments ($p < 0.001$), followed by LN and CH ($0.01 < p < 0.05$). RH was significantly increased by 78.64% and 74.78% under MG and HG, respectively, compared with NG ($p > 0.05$). Under MG, CH and CW increased by 31.86% and 88.77%, respectively, compared with NG. Correspondingly, LDW, LSFW, and LA were significantly increased by 44.45%, 38.12%, and 58.08%, respectively, under MG (Figure 2).

Compared with NG, the nine functional traits (except for LDW and LSFW in HG) showed negative deviation in *S. breviflora* under grazing conditions. In terms of the plasticity index (*PI*), it was found that RH, NH, CH, LDW, LSFW, LA, and CW varied more under MG than

FIGURE 1 Vegetation status of the plots after grazing under three grazing intensities (photographed August 9, 2020).

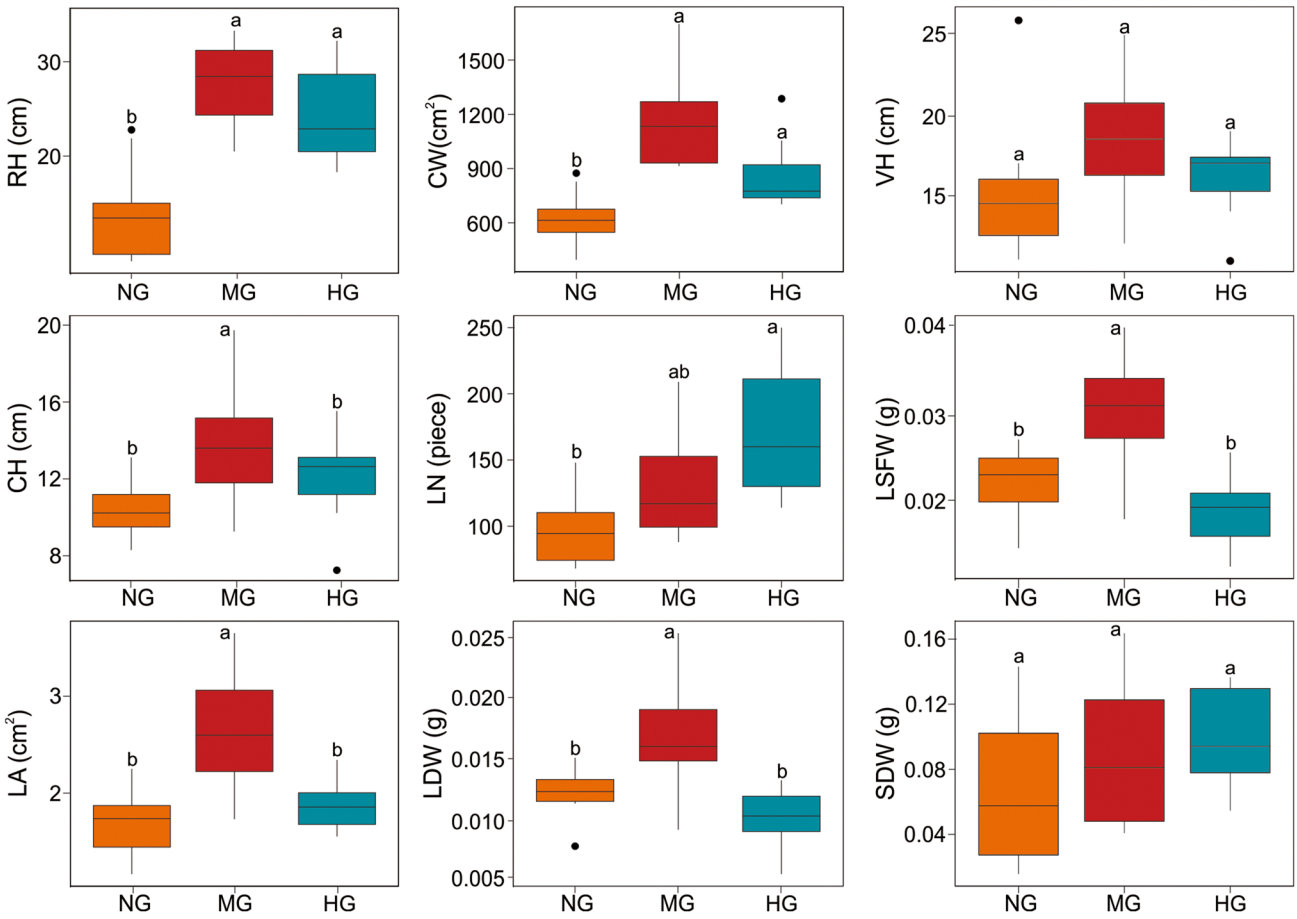

FIGURE 2 Functional traits of *Stipa breviflora* under different grazing intensities. The letter above the error bar indicates a significant difference ($p < 0.05$) between a comparison of two grazing treatments, and the values represent mean ± SE. The functional traits (reproductive tiller height, RH; clump width, CW; vegetative tiller height, VH; central height, CH; leaf number, LN; leaf saturated fresh weight, LSFW; leaf area, LA; leaf dry weight, LDW; and stem dry weight, SDW) for each grazing treatment represent the averages for 10 clusters of *S. breviflоris*. HG, heavy grazing; MG, moderate grazing; NG, no grazing.

under HG, and LN and SDW were higher under HG than under MG. Among all the traits, RH, LN, and CW showed the greatest *PI* deviations and can be regarded as the sensitivity indexes of *S. breviflora* in response to grazing (Table 1).

Photosynthetic physiology of *S. breviflora* under various grazing intensities

With increase in grazing intensity, P_n, G_s, and E significantly increased ($p < 0.05$) in *S. breviflora*, with the pattern of HG > MG > NG. However, C_i ($p > 0.05$) showed no significant increase under MG but a significant increase under HG (Figure 3).

Transcriptome sequencing, de novo assembly, and gene quantification and annotation

After sequencing, 56.94 GB clean data at the Q20 level (an error probability of 1%) were obtained in nine *S. breviflora* samples. The paired-end clean reads with a length of 150 bp for all samples were de novo assembled into 49 690–58 368 unigenes, with N50 values ranging from 1630 to 1812 bp. Further, the assembled unigenes of all samples were clustered into 124 728 all-unigenes, with an N50 of 2111 bp (Table S1). A BUSCO analysis revealed that the complete sequences of the finally assembled nonredundant transcriptome data set of *S. breviflora* accounted for 92.74% on comparing the 303 conserved sequences in the eukaryotic database,

indicating the integrity of the assembled transcriptome (Figure S1).

The gene quantification revealed that the overall expression patterns among the three replicates under NG and MG treatments were highly repeatable, whereas the HG3 sample showed substantial differences from the other two replicates (HG1 and HG2) of the HG treatment (Figure S2). Thus, the sample was excluded from the following analysis. Further, with a threshold of $CV \leq 0.7$ in the biological replicates of each grazing treatment and a mean TPM ≥ 1.0 in all analyzed samples, 34 552 all-unigenes were retained for subsequent analysis. Functional annotation revealed that 32 236 (93.30%) all-unigenes were obtained with at least one sequence match based on a BLAST search of public databases. Specifically, 31 746 (91.88%), 26 651 (77.13%), 26 367 (76.31%), 26 171 (75.74%), and 25 493 (73.78%) transcripts were annotated to NR, KEGG, GO, KOG, and Swiss-Prot databases, respectively (Table S2).

TABLE 1 Phenotypic *PI* of *Stipa breviflora* under two grazing intensities.

	MG		HG	
Traits	***PI***	***CV***	***PI***	***CV***
RH	−0.786	0.160	−0.748	0.176
VH	−0.211	0.202	−0.066	0.146
CH	−0.319	0.233	−0.150	0.186
LN	−0.346	0.326	−0.737	0.293
LDW	−0.445	0.285	+0.148	0.232
LSFW	−0.381	0.216	+0.146	0.214
SDW	−0.311	0.495	−0.493	0.293
LA	−0.581	0.226	−0.115	0.144
CW	−0.888	0.196	−0.366	0.207

Note: "−" and "+" indicate negative and positive deviation of functional traits, respectively.

Abbreviations: CH, central height; CV, coefficient of variation; CW, clump width; HG, heavy grazing; LA, leaf area; LDW, leaf dry weight; LN, leaf number; LSFW, leaf saturated fresh weight; MG, moderate grazing; PI, plasticity index; RH, reproductive tiller height; SDW, stem dry weight; VH, vegetative tiller height.

Identification, enrichment analysis, and prediction of subcellular localization of DEGs

Among the analyzed data set, 558 DEGs were identified via pairwise comparisons of the three grazing intensities (Figure 4b). Among them, 275 DEGs were identified in MG versus NG (153 upregulated and 122 downregulated), 212 in HG versus NG (88 upregulated and 124 downregulated), and 209 in HG versus MG (103 upregulated and 106 downregulated) (Figure 4a,b). GO enrichment analysis revealed that the DEGs were mainly enriched in chloroplast stroma (GO: 0009570), RNA binding (GO: 0003723), cytosol (GO: 0005829), and chloroplast (GO: 0009507) in the three main categories (molecular function, biological process, and cellular component) in GO database (Figure S3). In MG versus NG, the three most enriched terms were chloroplast stroma (GO:0009570), chloroplast (GO: 0009507), and

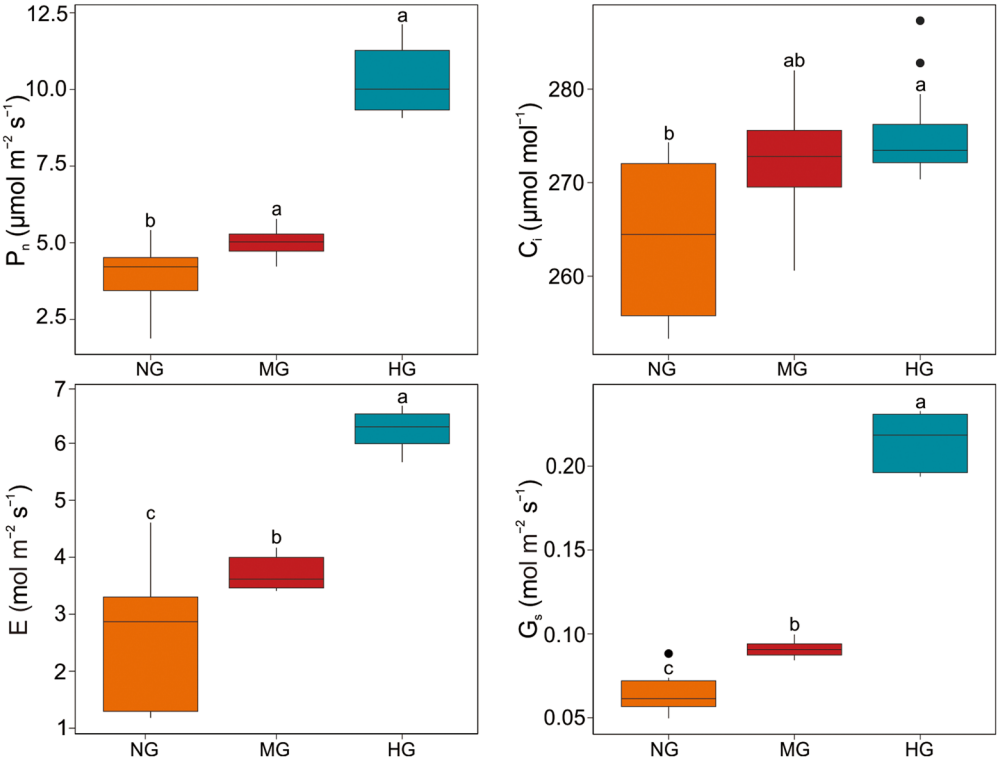

FIGURE 3 Photosynthetic characteristics of *Stipa breviflora* under various grazing treatments. The letter above the error bar indicates a significant difference ($p < 0.05$). The data are represented as mean ± SE. Grazing intensities are indicated as NG, MG, and HG. The photosynthetic physiological indexes (net photosynthetic rate, P_n; intercellular CO_2 concentration, C_i; transpiration rate, E; stomatal conductance, G_s) for each grazing treatment represent the averages for 10 clusters of *S. brevifloris*. HG, heavy grazing; MG, moderate grazing; NG, no grazing.

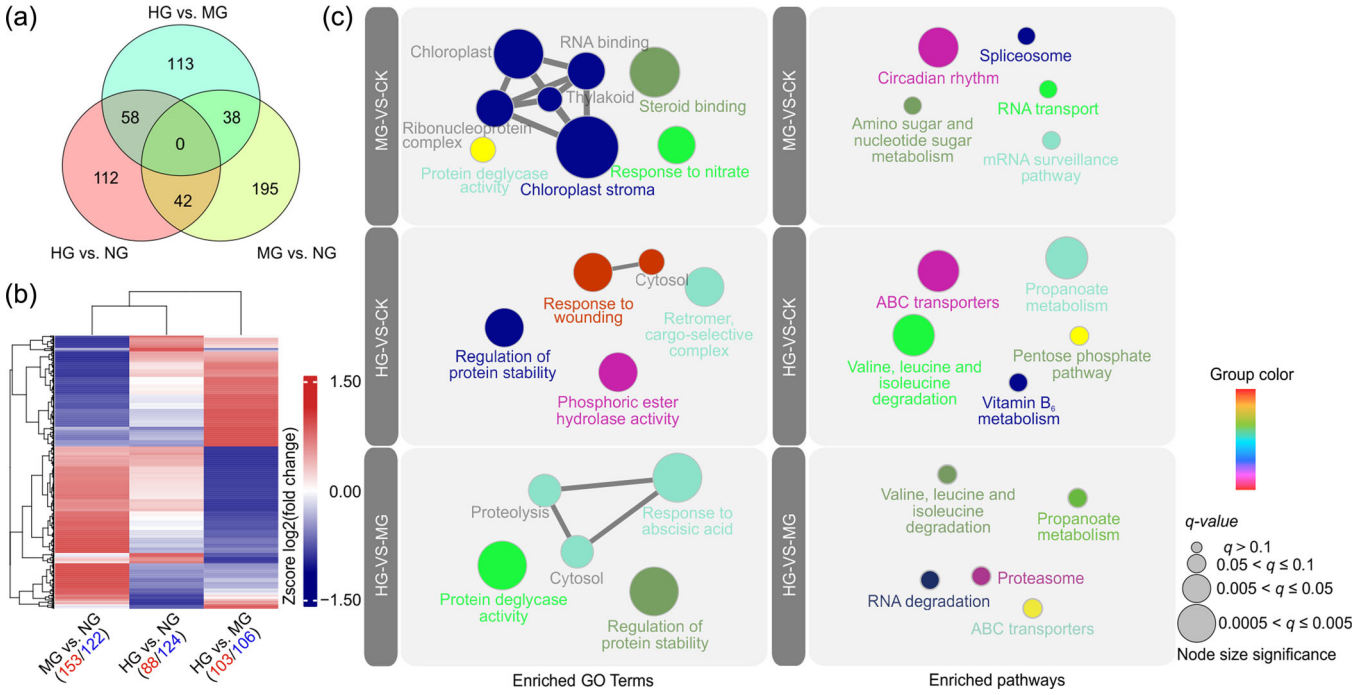

FIGURE 4 Expression profiling and enrichment analysis of the differentially expressed genes (DEGs). (a) Venn diagram of DEGs. (b) Cluster analysis of DEGs. (c) Gene Ontology (GO) and Kyoto Encyclopedia of Genes and Genomes (KEGG) enrichment analyses for the DEGs between two grazing intensities. DEGs contained in the most enriched ($q \leq 0.05$) GO terms and KEGG pathways were selected and visualized using ClueGo (version 2.5.9) and CluePedia (version 1.5.9). Grazing intensities are indicated as NG (no grazing), MG (moderate grazing), and HG (heavy grazing).

RNA binding (GO: 0003723). In HG versus NG and HG versus MG, cytosol (GO: 0005829) was the most enriched term (Figure 4c and Figure S4). KEGG enrichment analysis revealed that the DEGs were significantly enriched in RNA transport, circadian rhythm, and phenylpropanoid biosynthesis pathways (Figure S3). For MG versus NG, RNA transport, spliceosome, and mRNA surveillance pathway were relatively abundant. For HG versus NG and HG versus MG, valine, leucine, and isoleucine degradation; propanoate metabolism; ABC transporters; and pentose phosphate pathway were the most significantly enriched pathways (Figure 4c and Figure S4). Subcellular localization analysis revealed that of all the DEGs, 527 (94.44%) were assigned to certain cellular parts, and the three most dominant groups were genes related to chloroplast (34.76%), nucleus (23.11%), and cytosol (15.23%) (Figure S5).

Protein identification and quantification

A total of 729 266 spectra and 12 230 peptides were measured in the nine *S. breviflora* samples. The peptide length was approximately 7–17 amino acids (aa), among which the 9–12 aa interval was the peak area, accounting for 42.52% of all peptides. In total, 4455 proteins were identified under the criteria of FDR ≤ 1% (Table S3). *CV* analysis revealed that over 85% of the proteins had *CV* values <30%, indicating good reproducibility in repetitive samples (Figure S6). The molecular weight of the most identified proteins (75.82%) ranged from 10 to 60 aa (Figure S7), and proteins with the coverage of 1%–40% accounted for 94.19% of all proteins (Figure S8).

Identification, enrichment analysis, and prediction of subcellular localization of DEPs

A total of 541 DEPs were identified among the grazing treatments (Figure 5b). Of all DEPs, 253 were identified in MG versus NG (203 upregulated and 50 downregulated), 110 in HG versus NG (48 upregulated and 62 downregulated), and 419 in HG versus MG (325 upregulated and 94 downregulated) (Figure 5a,b). GO enrichment analysis revealed that the DEPs were mainly annotated to binding (GO: 0005488), monooxygenase activity (GO: 0004497), carbon fixation (GO: 0015977), and nucleus (GO: 0005634) in the three main GO categories (Figure S9). For MG versus NG, the DEPs were predominantly enriched in GO terms such as the integral component of the membrane (GO: 0016021), spliceosomal small nuclear ribonucleoprotein complex (GO: 0097525), and chlorophyll binding (GO: 0016168). For HG versus NG, the DEPs were mainly enriched in regulation of meristem growth (GO: 0010075), mitochondrial respiratory chain complex I (GO: 0005747), and regulation of transcription (GO: 0010630). For MG versus HG, the DEPs were predominantly enriched in mitochondrial respiratory chain complex I (GO: 0005747), reductive pentose-phosphate cycle (GO: 0019253), and negative regulation of defense response (GO: 0031348) (Figure 5c and Figure S10). KEGG enrichment analysis revealed that 464 DEPs were enriched in 102 KEGG pathways (Figure S9). In

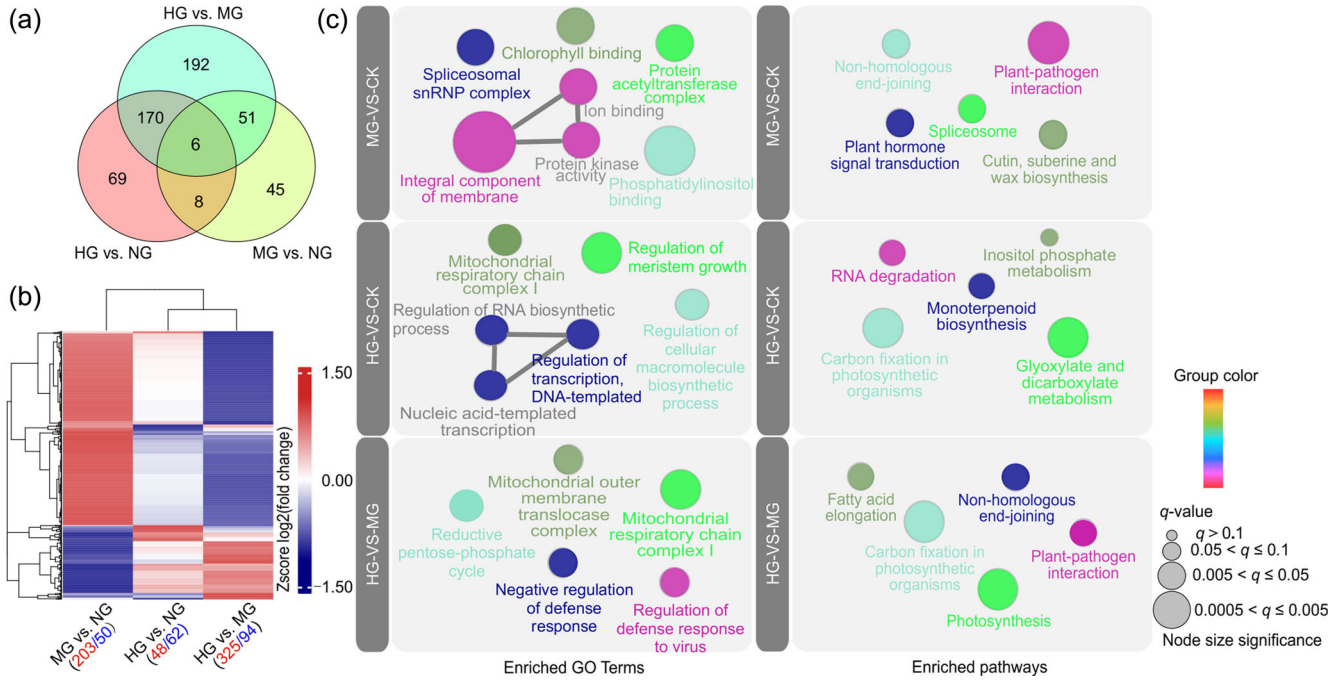

FIGURE 5 Expression profiling and enrichment analysis of differentially expressed proteins (DEPs). (a) Venn diagram of DEPs. (b) Cluster analysis of DEPs. (c) Gene Ontology (GO) and Kyoto Encyclopedia of Genes and Genomes (KEGG) enrichment analyses for the DEPs between two grazing intensities. DEPs contained in the most enriched ($q \leq 0.05$) GO terms and KEGG pathways were selected and visualized using ClueGo (version 2.5.9) and CluePedia (version 1.5.9). Grazing intensities are indicated as NG (no grazing), MG (moderate grazing), and HG (heavy grazing).

MG versus NG, spliceosome and plant–pathogen interaction pathways were the most enriched. In HG versus NG and MG versus HG, the DEPs were mainly enriched in carbon fixation in photosynthetic organisms and photosynthesis and glyoxylate and dicarboxylate metabolism. In MG versus HG, the DEPs were predominantly enriched in the phenylpropanoid biosynthesis pathway (Figure 5c and Figure S10). Subcellular localization analysis revealed that of all DEPs, 540 (99.814%) were assigned to certain cellular parts, and the three most predominant groups were DEPs related to chloroplast (37.52%), cytosol (29.39%), and nucleus (14.6%) (Figure S11).

Correlation analysis of the transcriptome and proteome

The combined analysis of the transcriptome and proteome of *S. breviflora* under various grazing treatments revealed that in MG versus NG, HG versus NG, and HG versus MG, 2735, 2815, and 2875 proteins/genes, respectively, were assigned to nine quadrants (Figure 6a–c). In general, only a small portion of the correlated transcripts and proteins showed significant positive or negative correlations (quadrants 1 and 9, as well as 3 and 7). However, most of the associated transcripts and proteins were differentially expressed at the transcriptome level (quadrants 2 and 8) or the proteome level (quadrants 4 and 6) (Figure 6a–c). Enrichment analysis revealed that the expression-correlated DEGs and DEPs, as well as the DEGs and DEPs that were differentially expressed at only one omic level, were enriched in GO terms and/or KEGG pathways associated with carbon metabolism and secondary metabolite biosynthesis such as chloroplast, cytosol, photosynthesis, and phenylpropanoid (Figure 6f,g). These biological processes or metabolic pathways may be closely associated with the response of *S. breviflora* to damage due to grazing, growth recovery, and defense mechanisms.

DEG/DEPs related to phenylpropanoid metabolism

A significant enrichment of DEGs/DEPs in the phenylpropanoid biosynthesis pathway was identified (Figure 7 and Table S4). This pathway involves enzymes such as phenylalanine ammonia-lyase (PAL), 4-coumarate–CoA ligase (4CL), *trans*-cinnamate 4-monooxygenase (C4H), cinnamoyl-CoA reductase (CCR), cinnamoyl alcohol dehydrogenase (CAD), peroxidase (POD), and ferulate 5-hydroxylase (F5H). Among these enzymes, DEGs encoding PAL (CL13827.Contig23_All), C4H (CL7463.Contig6_All), 4CL (Unigene1256_All), and F5H (CL6399.Contig2_All) were downregulated under MG but upregulated under HG. Compared with NG, CCR (CL4189.Contig4_All) was significantly upregulated under MG but downregulated under HG. Different POD-related DEGs showed three expression patterns. PODs (CL8091.Contig1_All and CL5808.Contig2_All) were upregulated under MG and downregulated under HG; POD (CL5308.Contig8_All) showed a continuous increase with grazing intensities. PODs (CL9961.Contig3_All, CL8302.Contig4_All, and CL8004.Contig2_All) were downregulated under MG and upregulated under HG. The C4H (tr|A0A446Q3U3|) and

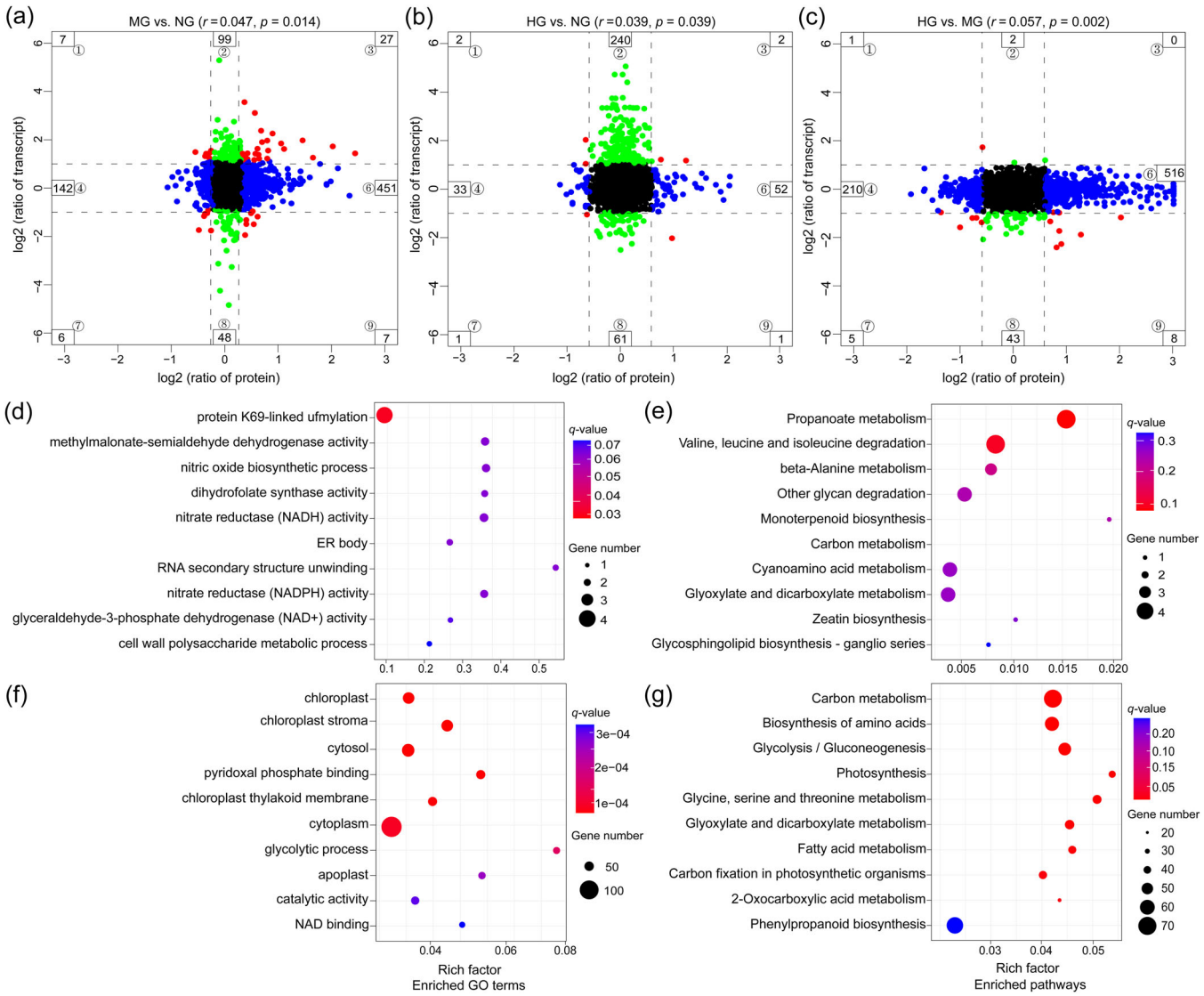

FIGURE 6 Transcriptome–proteome correlation analysis and functional enrichment analysis of *Stipa breviflora* under various grazing intensities. Scatter plots (a–c) represent the correlation analysis of transcripts and proteins in the nine quadrants. The *x*- and *y*-axis represent the fold change in protein and transcript levels [$\log_2$ (fold change)], respectively. Circles 1–9 indicate the quadrant numbers, and the numbers within the squares represent the number of correlated transcripts and proteins. Bubble plots (d and f) indicate the Gene Ontology (GO) enrichment analysis results for the correlated transcripts and proteins in quadrants 1, 9, 3, and 7 and quadrants 2, 8, 4, and 6, respectively. Bubble plots (e and g) represent the Kyoto Encyclopedia of Genes and Genomes (KEGG) enrichment analysis results for the correlated transcripts and proteins in quadrants 1, 9, 3, and 7 and quadrants 2, 8, 4, and 6, respectively. The size of the bubbles indicates the number of transcripts/proteins in the enriched GO terms and KEGG pathways, and the color represents the q value of enriched transcripts or proteins. Grazing intensities are indicated as NG (no grazing), MG (moderate grazing), and HG (heavy grazing).

CCR (tr|A0A0B5EBL5|) proteins were upregulated under MG and HG conditions compared with NG. CAD (tr|I1I1X8|) was significantly downregulated under MG but upregulated under HG. PODs (tr|A0A453APL7| and tr|A0A3B6SHD7|) showed an increasing trend with the grazing intensities, whereas PODs (tr|A0A0Q3H376|, tr|A0A446LP13|, tr|A0A446YUR1|, tr|A0A1D5UL37|, tr|A0A453APM5|, tr|M0Y0D4|, tr|I1GR63|, and tr|I1HF22|) were upregulated under MG and downregulated under HG.

Photosynthesis-associated DEGs/DEPs

The identified DEGs and DEPs were significantly enriched in metabolic pathways related to photosynthesis, including rbcS, photosystem II (PSII), glyceraldehyde-3-phosphate dehydrogenases (GAPDHases), cytochrome b6f (Cytb6f), thioredoxin, ferredoxin (Fd), and ATP synthase. Distinct expression patterns were observed under various grazing intensities (Figure 8 and Table S5). The rbcSs (tr|M8AQ24, tr|M7YD23), GAPDHase (tr|A0A446MF32), PSIIs (tr|H6BDG6, tr|A0A446KDG4, tr|M8A4S9, tr|Q40065, tr|I1GQI0, tr|A0A453N6V3, tr|A0A218L9M4, tr|A0A218LVT5, tr|A0A3B6H4W6), and photosystem I (PSI) (tr|A0A452XCG8) were upregulated under MG and downregulated under HG, although they altered to varying degrees. Notably, the highly expressed (TPM ≥ 100.0) PSII (CL4643.Contig2_All) and PSI (CL3162.Contig3_All) genes were significantly downregulated under grazing conditions, particularly under MG. Cytb6fs (tr|A0A287HT89, tr|A0A453PTL2, and tr|A0A218LZS6)

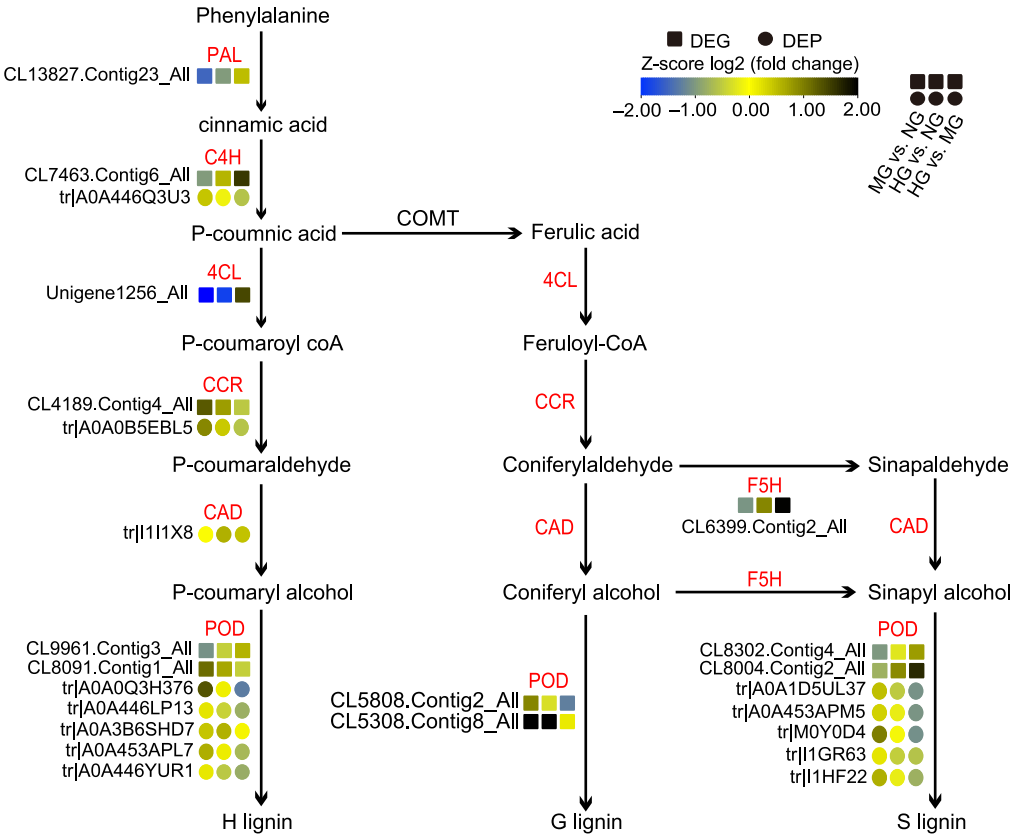

FIGURE 7 Expression patterns of differentially expressed genes/differentially expressed proteins (DEGs/DEPs) in the phenylpropanoid metabolic pathway. The heat map next to each enzyme represents the expression profiles of the DEGs and DEPs shown in Table S4. The circle and the square represent DEP and DEG, respectively. The abscissa is indicated from left to right: MG versus NG, HG versus NG, and MG versus HG. CAD, cinnamoyl alcohol dehydrogenase; CCR, cinnamoyl-CoA reductase; C4H, *trans*-cinnamate 4-monooxygenase; F5H, ferulate 5-hydroxylase; HG, heavy grazing; MG, moderate grazing; NG, no grazing; PAL, phenylalanine ammonia-lyase; 4CL, 4-coumarate–CoA ligase.

were upregulated under MG but significantly downregulated under HG (approximately 0.58 times that of MG). Thioredoxin (tr|A0A0Q3HXD0) was upregulated under MG but downregulated under HG. Moreover, the abundance of Fd (tr|I1GL62) significantly increased by approximately 1.56-fold under HG compared with MG. In contrast, the abundance of ATP synthase (CL4704.Contig6_All) decreased as the grazing intensity increased and was significantly downregulated under HG (approximately 0.49 times that of MG). ATP synthases (CL7658.Contig1_All, tr|A0A3G1AZ27, and tr|A0A446LLL7) showed significant upregulation, 1.4–5-fold, in MG compared with NG. However, under HG, ATP synthases were significantly downregulated by approximately 0.19–0.86-fold compared with MG. For thioredoxin, CL7849.Contig1_All was highly expressed in *S. breviflora* (TPM ≥ 100.0). It was significantly upregulated by threefold under MG compared with NG but downregulated under HG by 0.65-fold the expression level under MG.

Validation of DEPs

In total, 35 DEPs were validated using the PRM method. The PRM results demonstrated overall consistency with the quantitative findings obtained through IBT analysis and showed a consistent expression pattern for these proteins between the years 2020 and 2022 (Figure 12S).

DISCUSSION

Morphological and photosynthetic physiological phenotypes changed in *S. breviflora* under different grazing intensities

Functional traits of grassland plants are synergistically changed under long-term grazing disturbances (Carrasco et al., 2017). In this study, traits including RH, VH, and CW were significantly increased under MG compared with NG ($p < 0.05$). CH, CW, LDW, LSFW, and LA significantly decreased under HG ($p < 0.05$) compared with MG (Figure 2). This finding aligns with the compensatory growth model proposed by Belsky, specifically the concept of overcompensatory growth. When plants experience disturbances such as grazing or other damage, the accumulation of plant biomass may be stimulated, surpassing the net accumulation of undamaged plants, and thus promoting overall plant growth. In contrast, equity-compensatory growth occurs when the net accumulation of plant biomass is consumed or damaged, having minimal impact on the plant's growth (Belsky, 1986). For instance, an investigation into the

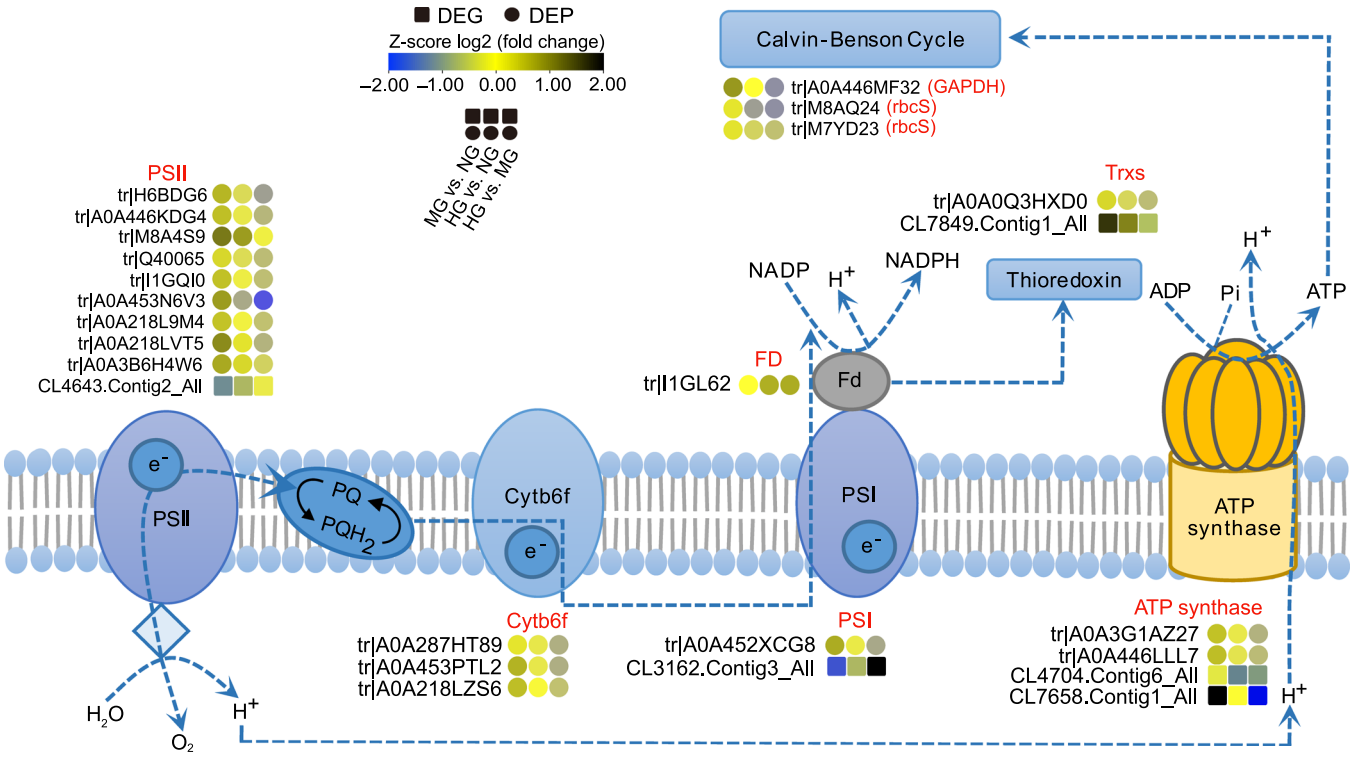

FIGURE 8 Expression patterns of differentially expressed genes/differentially expressed proteins (DEGs/DEPs) in the photosynthetic electron transport chain pathway. The heat map next to each enzyme represents the expression profiles of the DEGs and DEPs shown in Table S5. The circle and the square represent DEPs and DEGs, respectively. The abscissa is indicated from left to right: MG versus NG, HG versus NG, and MG versus HG. Cytb6f, cytochrome b6f; HG, heavy grazing; MG, moderate grazing; NG, no grazing; PSI, photosystem I; PSII, photosystem II.

aboveground net primary growth of four species of desert grassland plants (*Leymus secalinus*, *Stipa bungeana*, and *C. squarrosa*) under varying grazing intensities revealed that these plants showed overcompensatory growth in response to grazing disturbances. The reduction of grazing intensity facilitated the emergence of both super- and equal-compensatory growth (Ma & Xie, 2008). These results suggest that overcompensatory growth is evident in *S. breviflora* under MG conditions, reinforcing the idea that MG is beneficial for enhancing pasture regeneration capacity. In this study, the investigated functional traits of *S. breviflora* showed significant variation with increasing grazing intensity (Table 1). The *PI*s of the functional traits suggested that they can be used as phenotypic indicators of *S. breviflora* in response to grazing, particularly for RH, LN, and CW. In addition, the varying degrees in the plasticity of functional traits in *S. breviflora* may be due to the different sensitivity of functional traits to grazing disturbance. This can change its biological functions such as growth, reproduction, and defense, showing trade-offs among traits, which may be the adaptation strategy of this plant in response to grazing disturbance (Guo et al., 2017).

Photosynthesis is a determining factor of plant productivity (Flexas & Carriquí, 2020; Li et al., 2021; Ma et al., 2021). According to a previous study on the diurnal dynamics of photosynthesis in *S. breviflora*, the plants showed the peak electron transfer rate, Rubisco enzyme activity, photosynthetic rate, E, G_s, and the C_i between 09:00 a.m. and 10:00 a.m. These findings suggested that this period is the most active phase of photosynthesis for *S. breviflora* (Lei et al., 2021). In our study, we measured the photosynthetic physiological indicators around this period and observed differences in photosynthesis among *S. breviflora* plants under different grazing intensities. This suggests that the plant has developed distinct growth and development patterns under various grazing intensities.

After grazing, forage grasses undergo two stages of physiological changes, namely, short-term physiological damage and long-term physiological adjustments. The former occurs immediately after animal grazing and lasts for a maximum of 2 days, whereas the latter can persist for several weeks. During the long-term physiological adjustment stage, plants enhance their photosynthetic rate and photosynthesis to increase assimilate accumulation, promote compensatory growth of forage grasses, and adapt to the decrease in LA caused by grazing stress (Hou et al., 2002). Although grazing leads to damage to photosynthetic organs and a decrease in cellular contents of forage grasses, the reduction in vegetation cover in grazing areas indirectly improves land moisture retention and light transmission through the sparse canopy, thereby facilitating photosynthetic recycling. The regrowth after grazing mainly consists of tender leaves with strong photosynthetic capacity, which effectively elicits a positive response of forage grasses to grazing and promotes compensatory growth (Yuan et al., 2020; Zhu et al., 2013). The P_n, E, and G_s of *L. chinensis*, a typical grassland species, increased with increasing grazing intensities (Mi et al., 2015). This is consistent with our study. The three photosynthetic physiological indexes of *S. breviflora*

showed the same trend with increasing grazing intensity (Figure 3). Additionally, the number of leaves and stem biomass also increased with increasing grazing intensity (Figure 3). Therefore, these traits collectively contributed to biomass accumulation in *S. breviflora* after grazing and formation of phenotypic adaptive characteristics under long-term grazing stress.

Transcriptome and proteome of *S. breviflora* unsynergistically responded to grazing stress

Transcriptome and proteome represent different stages of gene expression. Many studies have reported that analysis of changes in either the transcriptome or the proteome alone is not sufficient to understand the functional patterns of genes in specific physiological states, life processes, stress adaptations, and other processes (Lou et al., 2018; Zhang et al., 2019; Zhu et al., 2022). However, a combined analysis of the transcriptome and the proteome provides a more comprehensive understanding of the plant's interaction with environmental changes and provides more reliable information for revealing related molecular mechanisms (Zhang et al., 2019). In this study, we performed RNA-Seq- and IBT-based quantitative analyses to identify the key DEGs and DEPs involved in the response of *S. breviflora* to grazing stress. The results revealed that the co-expression pattern between the transcriptome and the proteome was relatively low under grazing disturbance, suggesting a large-scale regulation of gene expression at the posttranscriptional and translational levels in this plant under different grazing intensities. This was consistent with previous findings (Ding et al., 2020; Lou et al., 2018). For instance, a comparative analysis of the transcriptome and proteome of *Eriobotrya japonica* revealed that out of 3620 genes, only 27 DEGs showed synergistic changes at the protein level, which were closely related to its cold-tolerance characteristics (Lou et al., 2018). In *S. breviflora*, uncorrelated levels of DEGs and DEPs were mainly associated with the key enzymes involved in photosynthesis, phenylpropanoid metabolism, and glutathione metabolism, and they may provide clues for exploring the relevant molecular mechanisms underlying the response of this species to grazing.

Plant-defense-associated DEGs/DEPs contributed to the adaptation to grazing by *S. breviflora*

Herbivory by grazing animals causes mechanical damage to grasses and triggers cascading biotic and abiotic stresses. In the process of wound healing in plants, lignin plays a significant role, and its increased accumulation accelerates plant damage repair and enhances mechanical defense capabilities. Regarding grazing avoidance in grasses, the accumulation of the aforementioned compounds reduces palatability, increases difficulty to digest, and consequently reduces the frequency of grass consumption (Zhao & Dixon, 2011).

Phenylpropanoid biosynthesis and metabolism play a crucial role in plant defense against biotic and abiotic stresses (Tato et al., 2013). By upregulating the enzymes of the phenylpropanoid biosynthetic pathway, plants produce polyphenolic compounds such as phenolic acids, flavonoids, and lignin, which contribute to stress tolerance and defense against pathogens (Shafi et al., 2015). The phenylpropanoid metabolism is initiated with three enzymatic reactions catalyzed by PAL, C4H, and 4CL. These reactions generate *p*-coumaroyl-CoA, which serves as a common precursor for the branch pathway of flavonoid synthesis composed of chalcone synthase (CHS) and chalcone isomerase (CHI) (Zhang et al., 2016). Additionally, feruloyl-CoA, synthesized from *p*-coumaroyl-CoA by C4H, is a key precursor in the monolignol synthesis pathway. After grazing, *S. grandis* and *L. chinensis* produce a large amount of secondary metabolites, including total flavonoids, phenols, and lignin, with leaves being the main synthesis and storage organs (Li et al., 2020). In *S. breviflora*, *PAL* (CL13827.Contig23_All), *C4H* (CL7463.Contig6_All), and *4CL* (Unigene1256_All) were slightly downregulated under MG but significantly upregulated under HG. C4H (tr|A0A446Q3U3|) was significantly upregulated after grazing, particularly in MG. CHS and CHI3 in the flavonoid metabolism pathway were significantly downregulated in MG but significantly upregulated under HG. Therefore, it is suggested that *S. breviflora* can enhance the synthesis of relevant metabolites by increasing the enzyme activities of PAL, C4H, and 4CL. In this way, wound healing after grazing is promoted in *S. breviflora*, enabling it to develop specific tolerance and avoidance responses to grazing.

The downstream regulation of lignin synthesis primarily involves the enzymes CCR and CAD. In *S. breviflora*, the thickness of leaf sclerenchyma tissue showed a trend of initially decreasing and then increasing with the increase of grazing intensity. The cell walls of thick-walled tissue contain lignin. This may be related to the grazing avoidance strategy of plants (Sachura. et al., 2023). Compared with NG, CCR (CL4189.Contig4_All, tr|A0A0B5EBL5|) in *S. breviflora* was significantly upregulated by approximately 2.38- and 1.91-fold under MG and approximately 1.64- and 1.34-fold under HG. CAD (tr|I1I1X8|) was slightly downregulated under MG and significantly upregulated by 1.53-fold under HG. This indicated that CCR and CAD were both positively regulated under HG and promote lignin synthesis and secondary cell wall thickening in postgrazing plants, thereby facilitating rapid wound repair and reducing mechanical damage caused by grazing.

F5H is another key enzyme involved in lignin synthesis and plays a critical regulatory role in syringyl lignin (S lignin) biosynthesis. Studies have reported that in transgenic tobacco and F5H-overexpressing *Arabidopsis*, the content of S lignin significantly increased, whereas the biosynthesis of G lignin was significantly inhibited (Franke et al., 2000; Sibout et al., 2002). In addition, changes in the content and composition of lignin affect the physicochemical properties of plants. When the ratio of S lignin to G lignin changes, it affects the induction levels of inducible and defense genes in plants, leading to the expression of more defense genes in plants with a higher content of guaiacyl units (Gallego-Giraldo et al., 2018). In *S. breviflora*, F5H (CL6399.Contig2_All) was downregulated under MG and

significantly upregulated by approximately 3.9-fold under HG. This suggested its possible involvement in regulating the S/G lignin ratio and influencing postgrazing growth, as well as inducing other defense genes to enhance the grazing adaptability of grazed *S. breviflora*.

The POD activity in plants such as *Ceratoides latens*, *Artemisia frigida*, *S. breviflora*, *Saussurea simpsoniana*, and *Oxytropis glabra* significantly increased under HG (Aodeng, 2004; Xiu, 2015). In the present study, the expression patterns of different PODs varied under different grazing conditions. These differential expressions of PODs suggested that this gene family serves as a sensitive factor in the response of *S. breviflora* to grazing, playing a role in the clearance of accumulated free radicals under grazing stress. Among them, POD (CL9961.Contig3_All) was highly expressed (mean TPM: 72); the POD (CL5308.Contig8_All, tr|A0A0Q3H376, tr|M0Y0D4) level significantly increased by two- to fivefold under MG and by one- to sixfold under HG, indicating that POD significantly regulated phenylpropanoid metabolism under different grazing intensities.

After assessing the expression patterns of genes and proteins in the phenylpropanoid metabolism pathway of *S. breviflora*, the transcript and protein levels of many genes (e.g., C4H and POD) showed discrepancies. This suggests a high sensitivity of the pathway to grazing stress in the species, involving nuanced regulation of both gene expression and protein synthesis. The specifics of this regulation may be influenced by factors such as plant species, the type of stress, and environmental conditions (Zhu et al., 2022).

Plant growth-associated DEGs/DEPs contributed to the adaptation of *S. breviflora* to grazing

Grazing and trampling activities of livestock damage the aboveground parts of plants, exposing plant leaves to intense light and affecting photosynthesis (Liu et al., 2019). Under grazing conditions, light intensity exceeds the demand for carbon assimilation, making PSII sensitive to light stress and prone to damage (Aro et al., 1993; Liu et al., 2019b; Takahashi & Badger, 2011). In *S. breviflora*, PSII (tr|H6BDG6, tr|A0A446KDG4, tr|M8A4S9, tr|Q40065, tr|I1GQI0, tr|A0A453N6V3, tr|A0A218L9M4, tr|A0A218LVT5, tr|A0A3B6H4W6, and tr|B3SH89) and PSI (tr|A0A452XCG8) were induced under MG; however, they were slightly downregulated under HG. PSII (CL4643.Contig2_All) and PSI (CL3162.Contig3_All) showed higher abundance in the transcriptome of *S. breviflora* (TPM > 100), with a slight decrease after HG. Under HG, the expression of *PSII*- and *PSI*-related genes and proteins was downregulated, suggesting damage to the light system of *S. breviflora*. This may be a mechanism to alleviate photodamage caused by excess light energy through reduced light absorption. Furthermore, the electron transfer rate of *S. breviflora* might be increased under MG, leading to enhanced activity of PSII and improved photosynthetic capacity (Yan et al., 2013). Therefore, under grazing stresses, *S. breviflora* experiences varying degrees of light system stress. Compared with NG and HG, MG was more favorable for the growth and survival of *S. breviflora*, supporting the hypothesis of moderate disturbance.

After the addition of sheep saliva, ATP synthase beta chain protein was downregulated in rice (Fan et al., 2011). In *S. breviflora*, ATP synthase (CL4704.Contig6_All) expression decreased with increasing grazing intensity, showing significant downregulation (by approximately 0.49-fold) under HG compared with MG. On the other hand, ATP synthase (CL7658.Contig1_All, tr|A0A3G1AZ27, tr|A0A446LLL7) in *S. breviflora* was significantly upregulated by 1.4–5-fold under MG compared with NG but was significantly downregulated by approximately 0.19–0.86-fold under HG compared with MG. These results indicate that the ATP production efficiency of *S. breviflora* was the highest under MG and decreased under HG. This could be due to increased vegetation exposure and enhanced light intensity under HG, leading to damage to the light system and subsequently affecting the levels of photosynthesis-related proteins and ATP synthesis. Studies have confirmed that the rate of photodamage to PSII is influenced by ATP synthesis (Allakhverdiev et al., 2005), which is consistent with the findings of this study.

To prevent photodamage, higher plants have evolved various protective mechanisms (Bailey et al., 2004; DalCorso et al., 2008). These include the removal of reactive ROS to mitigate the oxidative damage caused by ROS (Zheng et al., 2022), as well as the generation of ATP through the cyclic electron transport (CET) chain for photodamage repair (Yamori et al., 2016). In the CET pathway, electrons cycle from Fd to the Cytb6f complex (Johnson, 2011; Shikanai, 2007), creating a transmembrane proton gradient that drives ATP synthesis (Ruban et al., 2012). In this study, Fd (tr|I1GL62|I1GL62_BRADI) increased with grazing intensities and showed a significant increase under HG (approximately 1.56-fold compared with MG). Under HG, Fd (tr|I1GL62)-dependent cyclic electron flow was higher than that under MG and NG. This indicated that HG enhanced the rate and capacity of Fd-mediated cyclic electron flow, thus improving the protection of the photosystem reaction centers. *S. breviflora* produces a large amount of ROS under grazing conditions, and the Fd-mediated water–water cycle is an effective pathway for ROS scavenging in chloroplast (Liu et al., 2019; Munekage et al., 2002). CET can suppress the generation of ROS (Laisk et al., 2010). These findings collectively reflect the crucial role of CET in defense against light-induced damage caused by stress, satisfying the demand for ATP by chloroplasts under adverse conditions (Lehtimäki et al., 2010; Makino et al., 2002). The similar trends in gene and protein expression related to PSII repair, Fd-mediated cyclic electron flow, and carbon fixation pathways suggested the synergistic effects of these photoprotective mechanisms in alleviating photoinhibition and safeguarding photosynthesis, representing an adaptive strategy of *S. breviflora* in response to grazing.

The dark reaction in photosynthesis utilizes ATP and NADPH generated by the light reaction to convert CO_2 and water into carbohydrates through the

Calvin–Benson cycle. This process involves multiple enzymes, including RuBisCo, dehydrogenases, and kinases, and the activity of these enzymes affects the CO_2 fixation process. In *S. breviflora*, the rbcS (tr|M8AQ24, tr|M7YD23) was upregulated under MG but was significantly downregulated (approximately 0.5–0.7 times that of MG) under HG. GAPDHase (tr|A0A446MF32) was significantly upregulated by 1.75-fold under MG but downregulated (by approximately 0.46-fold compared with MG) under HG. In *S. grandis*, coding genes of RuBisCo and GAPDHase were highly expressed under moderate and HG conditions, leading to overcompensatory growth and increased photosynthetic capacity under HG compared with MG (Dang et al., 2021). Similarly, *S. breviflora* showed a significant increase in the relative expression levels of RuBisCo and GAPDHase, as well as P_ns, under MG. This indicated that the relative expression of proteins directly affects the photosynthetic process in the species by enhancing photosynthesis to meet energy requirements for survival under MG conditions. However, under HG, the relative expression levels of RuBisCo and GAPDHase did not correlate with the P_n index. This may be attributed to the better-maintained photosynthetic transmission system and normal metabolic cycles in the leaves under MG. As the grazing intensity increases, the degree of damage to the photosynthetic system intensifies. This results in the inhibition of photosynthetic metabolism, and consequently, the expression of RuBisCo and GAPDHase shows corresponding changes.

CONCLUSIONS

Long-term grazing led to molecular phenotypic plasticity, influencing various biological processes and metabolic pathways in *S. breviflora*. Under different grazing intensities, 558 DEGs and 541 DEPs were identified in the species. They were mainly related to RNA processing, carbon metabolism, and secondary metabolite biosynthesis. Correlation analysis revealed low correlation between the transcriptome and the proteome. This indicated a large-scale regulation of gene expression at the posttranscriptional and translational levels during the response of plants to grazing. Expression profiles of the key genes and proteins involved in photosynthesis and phenylpropanoid metabolism pathways suggested their synergistic response to grazing in *S. breviflora*. This study enhances the understanding of the response mechanisms underlying the adaptation to grazing in grassland plants and provides valuable insights into the phenotypic and molecular adaptations of *S. breviflora* under long-term grazing. However, this study has some limitations. The present study analyzed *S. breviflora* samples at a single, although representative, time point under different grazing intensities; this may not reflect the exact conclusion, given the complex nature of the *S. breviflora*'s response to grazing. Diurnal variations and coordination at multiple levels of gene and protein expression and metabolite synthesis are involved under different grazing intensities. In subsequent studies, more time points need to be included to reveal the grazing adaptation mechanism of *S. breviflora*. Additionally, the majority of DEG- and DEP-related genes/enzymes identified in this study belong to gene families, and the specific member in relevant pathways involved in the grazing response was not identified. Future studies should focus on identifying the key genes, enzymes, and relevant metabolites that play specific roles in *S. breviflora* in response to grazing stress, thus revealing the molecular mechanisms underlying the grazing adaptation in this species.

AUTHOR CONTRIBUTIONS

Yanan Liu: Conceptualization; data curation; methodology; writing—original draft. **Shixian Sun**: Data curation; project administration; resources. **Yanan Zhang**: Data curation; investigation; methodology; validation. **Miaomiao Song**: Investigation. **Yunyun Tian**: Data curation; methodology; writing—review and editing. **Peter J. Lockhart**: Visualization; writing—review and editing. **Xin Zhang**: Investigation. **Ying Xu**: Investigation. **Zhenhua Dang**: Data curation; project administration; resources; visualization; writing—review and editing.

ACKNOWLEDGMENTS

We thank mjeditor (https://www.mjeditor.com) for editing the English text of a draft of this manuscript. This work was supported by the National Natural Science Foundation of China (32160088), the Program for Young Talents of Science and Technology in Universities of Inner Mongolia Autonomous Region of China (NJYT22093), and the Open Project Program of Ministry of Education Key Laboratory of Ecology and Resources Use of the Mongolian Plateau.

CONFLICT OF INTEREST STATEMENT

The authors declare no conflicts of interest.

DATA AVAILABILITY STATEMENT

The data that supports the findings of this study are available in the Supporting Information of this article.

REFERENCES

Allakhverdiev, S. I., Nishiyama, Y., Takahashi, S., Miyairi, S., Suzuki, I., & Murata, N. (2005). Systematic analysis of the relation of electron transport and ATP synthesis to the photodamage and repair of photosystem II in *Synechocystis*. *Plant Physiology*, *137*(1), 263–273. https://doi.org/10.1104/pp.104.054478

Aodeng, G. W. (2004). *The influence of stocking rate on plant community and eco-physiology of main plant populations in Stipa breviflora desert steppe* [Master's degree thesis, Inner Mongolia Agricultural University, Hohhot, Inner Mongolia, China]. https://kns.cnki.net/KCMS/detail/detail.aspx?dbname=CMFD9904&filename=2004076731.nh

Aro, E. M., Virgin, I., & Andersson, B. (1993). Photoinhibition of photosystem II. Inactivation, protein damage and turnover. *Biochimica et Biophysica Acta (BBA)—Bioenergetics*, *1143*, 113–134. https://doi.org/10.1016/0005-2728(93)90134-2

Bailey, S., Horton, P., & Walters, R. G. (2004). Acclimation of *Arabidopsis thaliana* to the light environment: The relationship between photosynthetic function and chloroplast composition. *Planta*, *218*(5), 793–802. https://doi.org/10.1007/s00425-003-1158-5

Belsky, A. J. (1986). Does herbivory benefit plants? A review of the evidence. *The American Naturalist*, *127*(6), 870–892. https://doi.org/10.1086/284531

Benot, M. L., Morvan-Bertrand, A., Mony, C., Huet, J., Sulmon, C., Decau, M. L., Prud'homme, M. P., & Bonis, A. (2019). Grazing intensity modulates carbohydrate storage pattern in five grass species from temperate grasslands. *Acta Oecologica*, *95*, 108–115. https://doi.org/10.1016/j.actao.2018.11.005

Bolger, A. M., Lohse, M., & Usadel, B. (2014). Trimmomatic: A flexible trimmer for Illumina sequence data. *Bioinformatics*, *30*(15), 2114–2120. https://doi.org/10.1093/bioinformatics/btu170

Carrasco, A., Wegrzyn, J. L., Durán, R., Fernández, M., Donoso, A., Rodriguez, V., Neale, D., & Valenzuela, S. (2017). Expression profiling in *Pinus radiata* infected with *Fusarium circinatum*. *Tree Genetics & Genomes*, *13*(2), 46. https://doi.org/10.1007/s11295-017-1125-0

Chen, S. Y., Li, X. Q., Zhao, A. G., Wang, L. J., Li, X. F., Shi, Q. Y., Chen, M., Guo, J., Zhang, J. C., Qi, D. M., & Liu, G. S. (2009). Genes and pathways induced in early response to defoliation in rice seedlings. *Current Issues in Molecular Biology*, *11*(2), 81–100. https://doi.org/10.21775/cimb.011.081

Chen, Y., Chen, Y., Shi, C., Huang, Z., Zhang, Y., Li, S., Li, Y., Ye, J., Yu, C., Li, Z., Zhang, X., Wang, J., Yang, H., Fang, L., & Chen, Q. (2018). SOAPnuke: A MapReduce acceleration-supported software for integrated quality control and preprocessing of high-throughput sequencing data. *GigaScience*, *7*(1), 1–6. https://doi.org/10.1093/gigascience/gix120

Conesa, A., Götz, S., García-Gómez, J. M., Terol, J., Talón, M., & Robles, M. (2005). Blast2GO: A universal tool for annotation, visualization and analysis in functional genomics research. *Bioinformatics*, *21*(18), 3674–3676. https://doi.org/10.1093/bioinformatics/bti610

Cui, X. Y., Guo, K., Hao, Y. B., & Chen, Z. Z. (2012). Degradation and management of steppes in China. In M. J. A. Weger & M. A. van Staalduinen (Eds.), *Eurasian steppes. Ecological problems and livelihoods in a changing world* (pp. 475–490). Springer. https://doi.org/10.1007/978-94-007-3886-718

DalCorso, G., Pesaresi, P., Masiero, S., Aseeva, E., Schünemann, D., Finazzi, G., Joliot, P., Barbato, R., & Leister, D. (2008). A complex containing PGRL1 and PGR5 is involved in the switch between linear and cyclic electron flow in *Arabidopsis*. *Cell*, *132*(2), 273–285. https://doi.org/10.1016/j.cell.2007.12.028

Dang, Z., Jia, Y., Tian, Y., Li, J., Zhang, Y., Huang, L., Liang, C., Lockhart, P. J., Matthew, C., & Li, F. Y. (2021). Transcriptome-wide gene expression plasticity in *Stipa grandis* in response to grazing intensity differences. *International Journal of Molecular Sciences*, *22*(21), 11882. https://doi.org/10.3390/ijms222111882

Ding, H., Mo, S., Qian, Y., Yuan, G., Wu, X., & Ge, C. (2020). Integrated proteome and transcriptome analyses revealed key factors involved in tomato (*Solanum lycopersicum*) under high temperature stress. *Food and Energy Security*, *9*(4), e239. https://doi.org/10.1002/fes3.239

Fan, W., Cui, W., Li, X., Chen, S., Liu, G., & Shen, S. (2011). Proteomics analysis of rice seedling responses to ovine saliva. *Journal of Plant Physiology*, *168*(5), 500–509. https://doi.org/10.1016/j.jplph.2010.08.012

Flexas, J., & Carriquí, M. (2020). Photosynthesis and photosynthetic efficiencies along the terrestrial plant's phylogeny: Lessons for improving crop photosynthesis. *The Plant Journal*, *101*(4), 964–978. https://doi.org/10.1111/tpj.14651

Franke, R., McMichael, C. M., Meyer, K., Shirley, A. M., Cusumano, J. C., & Chapple, C. (2000). Modified lignin in tobacco and poplar plants over-expressing the *Arabidopsis* gene encoding ferulate 5-hydroxylase. *The Plant Journal*, *22*(3), 223–234. https://doi.org/10.1046/j.1365-313x.2000.00727.x

Gallego-Giraldo, L., Posé, S., Pattathil, S., Peralta, A. G., Hahn, M. G., Ayre, B. G., Sunuwar, J., Hernandez, J., Patel, M., Shah, J., Rao, X., Knox, J. P., & Dixon, R. A. (2018). Elicitors and defense gene induction in plants with altered lignin compositions. *New Phytologist*, *219*(4), 1235–1251. https://doi.org/10.1111/nph.15258

Grabherr, M. G., Haas, B. J., Yassour, M., Levin, J. Z., Thompson, D. A., Amit, I., Adiconis, X., Fan, L., Raychowdhury, R., Zeng, Q., Chen, Z., Mauceli, E., Hacohen, N., Gnirke, A., Rhind, N., di Palma, F., Birren, B. W., Nusbaum, C., Lindblad-Toh, K., … Regev, A. (2011). Trinity: Reconstructing a full-length transcriptome without a genome from RNA-Seq data. *Nature Biotechnology*, *29*(7), 644–652. https://doi.org/10.1038/nbt.1883

Guo, H., Guan, L., Wang, Y., Xie, L., Prather, C. M., Liu, C., & Ma, C. (2017). Grazing limits natural biological controls of woody encroachment in Inner Mongolia steppe. *Biology Open*, *6*(10), 1569–1574. https://doi.org/10.1242/bio.026443

Hou, F. J., Li, G., & Chang, S. H. (2002). Physiological indices of grazed grassland under health management. *Chinese Journal of Applied Ecology*, *13*(8), 1049–1053. https://doi.org/10.13287/j.1001-9332.2002.0242

Jia, L. X., Yang, Y., Zhang, F., Qiao, J. R., & Zhao, M. L. (2019). Response in tiller numbers of *Stipa breviflora* to endogenous hormone concentration under different stocking rates. *Acta Ecologica Sinica*, *39*(7), 2391–2397. https://doi.org/10.5846/stxb201805271163

Johnson, G. N. (2011). Physiology of PSI cyclic electron transport in higher plants. *Biochimica et Biophysica Acta (BBA)—Bioenergetics*, *1807*(3), 384–389. https://doi.org/10.1016/j.bbabio.2010.11.009

Laisk, A., Talts, E., Oja, V., Eichelmann, H., & Peterson, R. B. (2010). Fast cyclic electron transport around photosystem I in leaves under far-red light: A proton-uncoupled pathway? *Photosynthesis Research*, *103*(2), 79–95. https://doi.org/10.1007/s11120-009-9513-4

Langmead, B., & Salzberg, S. L. (2012). Fast gapped-read alignment with Bowtie 2. *Nature Methods*, *9*(4), 357–359. https://doi.org/10.1038/nmeth.1923

Lehtimäki, N., Lintala, M., Allahverdiyeva, Y., Aro, E. M., & Mulo, P. (2010). Drought stress-induced upregulation of components involved in ferredoxin-dependent cyclic electron transfer. *Journal of Plant Physiology*, *167*(12), 1018–1022. https://doi.org/10.1016/j.jplph.2010.02.006

Lei, X. F., Wang, Y., Li, Y., Liang, Y., & Bai, L. (2021). Effects of long-term warming on photosynthesis daily dynamics of three main plants in *Stipa breviflora* desert steppe. *Journal of Northern Agriculture*, *49*(1), 111–118. https://doi.org/10.12190/j.issn.2096-1197.2021.01.16

Li, B., & Dewey, C. N. (2011). RSEM: Accurate transcript quantification from RNA-Seq data with or without a reference genome. *BMC Bioinformatics*, *12*, 323. https://doi.org/10.1186/1471-2105-12-323

Li, F., An, J. Y., Li, X. L., Ding, Y., Li, Y. H., & Bai, W. K. (2021). Asymmetrical response of aboveground and belowground traits of *Agropyron cristatum* to grazing intensities. *Chinese Journal of Grassland*, *43*(11), 18–25. https://doi.org/10.16742/j.zgcdxb.20210123

Li, J., Hou, F., & Ren, J. (2021). Grazing intensity alters leaf and spike photosynthesis, transpiration, and related parameters of three grass species on an alpine steppe in the Qilian mountains. *Plants*, *10*(2), 294. https://doi.org/10.3390/plants10020294

Li, X. L., Hou, X. Y., Wu, X. H., Ji, L., Chen, H. J., & Liu, Z. Y. (2014). Plastic responses of stem and leaf functional traits in Leymus chinensis to long-term grazing in a meadow steppe. *Chinese Journal of Plant Ecology*, *38*(5), 440–451. https://doi.org/10.3724/SP.J.1258.2014.00040

Li, Y., Gong, J. R., Liu, M., Hou, X. Y., Ding, Y., Yang, B., Zhang, Z. H., Wang, B., & Zhu, C. C. (2020). Defense strategies of dominant plants under different grazing intensity in the typical temperate steppe of Nei Mongol, China. *Chinese Journal of Plant Ecology*, *44*(6), 642–653. https://doi.org/10.17521/cjpe.2019.0329

Lienin, P., & Kleyer, M. (2012). Plant trait responses to the environment and effects on ecosystem properties. *Basic and Applied Ecology*, *13*(4), 301–311. https://doi.org/10.1016/j.baae.2012.05.002

Lisonbee, L. D., Villalba, J. J., & Provenza, F. D. (2009). Effects of tannin on selection by sheep of forages containing alkaloids, tannins and saponins. *Journal of the Science of Food and Agriculture*, *89*(15), 2668–2677. https://doi.org/10.1002/jsfa.3772

Liu, C., Dong, L. A., Lin, J. Z., & Liu, X. M. (2019). Research advances on regulation mechanism of reactive oxygen species metabolism under stresses. *Life Science Research*, *23*(3), 253–258. https://doi.org/10.16605/j.cnki.1007-7847.2019.03.012

Liu, M., Gong, J. R., Yang, B., Ding, Y., Zhang, Z. H., Wang, B., Zhu, C. C., & Hou, X. Y. (2019). Differences in the photosynthetic and physiological responses of *Leymus chinensis* to different levels of grazing intensity. *BMC Plant Biology*, *19*(1), 558. https://doi.org/10.1186/s12870-019-2184-1

Liu, S., Tang, Y., Zhang, F., Du, Y., Lin, L., Li, Y., Guo, X., Li, Q., & Cao, G. (2017). Changes of soil organic and inorganic carbon in relation to grassland degradation in Northern Tibet. *Ecological Research*, *32*(3), 395–404. https://doi.org/10.1007/s11284-017-1447-2

Liu, Z. Y., Zhang, Z., Zhang, T. Y., Gao, R. F., & Li, X. L. (2019). Heavy grazing effects on stem elongation and internode allometry: Insights from a natural pasture grass. *Grass and Forage Science*, *74*(3), 427–436. https://doi.org/10.1111/gfs.12416

Lou, X., Wang, H., Ni, X., Gao, Z., & Iqbal, S. (2018). Integrating proteomic and transcriptomic analyses of loquat (*Eriobotrya japonica* Lindl.) in response to cold stress. *Gene*, *677*, 57–65. https://doi.org/10.1016/j.gene.2018.07.022

Ma, H. B. (2008). Influence of different grazing intensities in desert steppe on some physiological indexes of several pastures. *Agricultural Research in the Arid Areas*, *26*(2), 79–84. https://doi.org/10.7606/j.issn.1000-7601.2008.02.16

Ma, H. B., & Xie, Y. Z. (2008). Plant compensatory growth under different grazing intensities in desert steppe. *Scientia Agricultura Sinica*, *41*(11), 3645–3650. https://doi.org/10.3864/j.issn.0578-1752.2008.11.026

Ma, Z., Bork, E. W., Li, J., Chen, G., & Chang, S. X. (2021). Photosynthetic carbon allocation to live roots increases the year following high intensity defoliation across two ecosites in a temperate mixed grassland. *Agriculture, Ecosystems & Environment*, *316*, 107450. https://doi.org/10.1016/j.agee.2021.107450

MacLean, B., Tomazela, D. M., Shulman, N., Chambers, M., Finney, G. L., Frewen, B., Kern, R., Tabb, D. L., Liebler, D. C., & MacCoss, M. J. (2010). Skyline: An open source document editor for creating and analyzing targeted proteomics experiments. *Bioinformatics*, *26*(7), 966–968. https://doi.org/10.1093/bioinformatics/btq054

Makino, A., Miyake, C., & Yokota, A. (2002). Physiological functions of the water–water cycle (Mehler reaction) and the cyclic electron flow around PSI in rice leaves. *Plant and Cell Physiology*, *43*(9), 1017–1026. https://doi.org/10.1093/pcp/pcf124

Mi, X., Li, X. B., Wang, H., Huang, Q., & Bai, Y. X. (2015). Photosynthetic ecophysiology characteristics of *Leymus chinensis* under different grazing intensities in Inner Mongolia steppe. *Chinese Journal of Grassland*, *37*(3), 92–98. https://www.doc88.com/p-9159555596150.html

Munekage, Y., Hojo, M., Meurer, J., Endo, T., Tasaka, M., & Shikanai, T. (2002). PGR5 is involved in cyclic electron flow around photosystem I and is essential for photoprotection in *Arabidopsis*. *Cell*, *110*(3), 361–371. https://doi.org/10.1016/S0092-8674(02)00867-X

Orwin, K. H., Mason, N. W. H., Jordan, O. M., Lambie, S. M., Stevenson, B. A., & Mudge, P. L. (2018). Season and dominant species effects on plant trait–ecosystem function relationships in intensively grazed grassland. *Journal of Applied Ecology*, *55*(1), 236–245. https://doi.org/10.1111/1365-2664.12939

Pertea, G., Huang, X., Liang, F., Antonescu, V., Sultana, R., Karamycheva, S., Lee, Y., White, J., Cheung, F., Parvizi, B., Tsai, J., & Quackenbush, J. (2003). TIGR Gene Indices clustering tools (TGICL): A software system for fast clustering of large EST datasets. *Bioinformatics*, *19*(5), 651–652. https://doi.org/10.1093/bioinformatics/btg034

Rotundo, J. L., & Aguiar, M. R. (2007). Herbivory resistance traits in populations of *Poa ligularis* subjected to historically different sheep grazing pressure in Patagonia. *Plant Ecology*, *194*(1), 121–133. https://doi.org/10.1007/s11258-007-9279-8

Ruban, A. V., Johnson, M. P., & Duffy, C. D. P. (2012). The photoprotective molecular switch in the photosystem II antenna. *Biochimica et Biophysica Acta (BBA)— Bioenergetics*, *1817*(1), 167–181. https://doi.org/10.1016/j.bbabio.2011.04.007

Sachura, Z. X., Zhu, L., Kangsaruul, S. S., Lu, X. R., & Xie, J. F. (2023). Leaf anatomical changes of *Stipa Breviflora* under long-term different grazing intensities in desert steppe. *Acta Ecologica Sinica*, *43*(14), 6005–6014. https://doi.org/10.5846/stxb202205161369

Shafi, A., Chauhan, R., Gill, T., Swarnkar, M. K., Sreenivasulu, Y., & Kumar, S. (2015). Expression of SOD and APX genes positively regulates secondary cell wall biosynthesis and promotes plant growth and yield in Arabidopsis under salt stress. *Plant Molecular Biology*, *87*(6), 615–631. https://doi.org/10.1007/s11103-015-0301-6

Shikanai, T. (2007). Cyclic electron transport around photosystem I: Genetic approaches. *Annual Review of Plant Biology*, *58*, 199–217. https://doi.org/10.1146/annurev.arplant.58.091406.110525

Sibout, R., Baucher, M., Gatineau, M., Van Doorsselaere, J., Mila, I., Pollet, B., Maba, B., Pilate, G., Lapierre, C., Boerjan, W., & Jouanin, L. (2002). Expression of a poplar cDNA encoding a ferulate-5-hydroxylase/coniferaldehyde 5-hydroxylase increases S lignin deposition in *Arabidopsis thaliana*. *Plant Physiology and Biochemistry*, *40*(12), 1087–1096. https://doi.org/10.1016/S0981-9428(02)01474-2

Simão, F. A., Waterhouse, R. M., Ioannidis, P., Kriventseva, E. V., & Zdobnov, E. M. (2015). BUSCO: Assessing genome assembly and annotation completeness with single-copy orthologs. *Bioinformatics*, *31*(19), 3210–3212. https://doi.org/10.1093/bioinformatics/btv351

Srinivasa, Y. B. (2018). Breaching plant defence theories: Growth rates of plants directly impact the evolution of consumption rates of herbivorous insects. *Current Science*, *114*, 258–260. https://doi.org/10.18520/cs/v114/i02/258-260

Takahashi, S., & Badger, M. R. (2011). Photoprotection in plants: A new light on photosystem II damage. *Trends in Plant Science*, *16*(1), 53–60. https://doi.org/10.1016/j.tplants.2010.10.001

Tato, L., De-Nisi, P., Donnini, S., & Zocchi, G. (2013). Low iron availability and phenolic metabolism in a wild plant species (*Parietaria judaica L.*). *Plant Physiology and Biochemistry*, *72*, 145–153. https://doi.org/10.1016/j.plaphy.2013.05.017

Thimm, O., Bläsing, O., Gibon, Y., Nagel, A., Meyer, S., Krüger, P., Selbig, J., Müller, L. A., Rhee, S. Y., & Stitt, M. (2004). MAPMAN: A user-driven tool to display genomics data sets onto diagrams of metabolic pathways and other biological processes. *The Plant Journal*, *37*(6), 914–939. https://doi.org/10.1111/j.1365-313X.2004.02016.x

Wan, D., Wan, Y., Hou, X., Ren, W., Ding, Y., & Sa, R. (2015). De novo assembly and transcriptomic profiling of the grazing response in *Stipa grandis*. *PloS One*, *10*(4), e0122641. https://doi.org/10.1371/journal.pone.0122641

Wang, C., Jian, S., Ren, H., Yan, J., & Liu, N. (2021). A web-based software platform for restoration-oriented species selection based on plant functional traits. *Frontiers in Ecology and Evolution*, *9*, 570454. https://doi.org/10.3389/fevo.2021.570454

Wang, J., Zhao, Y., Ray, I., & Song, M. (2016). Transcriptome responses in alfalfa associated with tolerance to intensive animal grazing. *Scientific Reports*, *6*, 19438. https://doi.org/10.1038/srep19438

Wen, B., Zhou, R., Feng, Q., Wang, Q., Wang, J., & Liu, S. (2014). IQuant: An automated pipeline for quantitative proteomics based upon isobaric tags. *Proteomics*, *14*, 2280–2285. https://doi.org/10.1002/pmic.201300361

Xing, X. Q., Zhang, L., Taogetao, B. Y., & Yang, Z. P. (2019). Effect of grazing on the aboveground functional traits of *Cleistogenes squarrosa*. *Chinese Journal of Grassland*, *41*(6), 116–122. https://doi.org/10.16742/j.zgcdxb.20190115

Xiu, H. (2015). Changes of protective enzyme activity and MDA content in leaves of *Agropyron cristatum* under grazing stress. *Agricultural Science and Technology*, *16*(1), 22–24, 39. https://doi.org/10.16175/j.cnki.1009-4229.2015.01.009

Yamori, W., Makino, A., & Shikanai, T. (2016). A physiological role of cyclic electron transport around photosystem I in sustaining photosynthesis under fluctuating light in rice. *Scientific Reports*, *6*, 20147. https://doi.org/10.1038/srep20147

Yan, X., Gong, J. R., Zhang, Z. Y., Huang, Y. M., An, R., Qi, Y., & Liu, M. (2013). Responses of photosynthetic characteristics of *Stipa baicalensis* to grazing disturbance. *Chinese Journal of Plant Ecology*, *37*(6), 530–541. https://doi.org/10.3724/SP.J.1258.2013.00054

Yu, S., Jiang, L., Du, W., Zhao, J., Zhang, H., Zhang, Q., & Liu, H. (2020). Estimation and spatio-temporal patterns of carbon emissions from grassland fires in Inner Mongolia, China. *Chinese Geographical Science*, *30*(4), 572–587. https://doi.org/10.1007/s11769-020-1134-z

Yuan, J., Li, H., & Yang, Y. (2020). The compensatory tillering in the forage grass *Hordeum brevisubulatum* after simulated grazing of different severity. *Frontiers in Plant Science*, *11*, 792. https://doi.org/10.3389/fpls.2020.00792

Zhang, H., Fu, Y., Guo, H., Zhang, L., Wang, C. Y., Song, W. N., Yan, Z. G., Wang, Y. J., & Ji, W. Q. (2019). Transcriptome and proteome-based network analysis reveals a model of gene activation in wheat resistance to stripe rust. *International Journal of Molecular Sciences*, *20*(5), 1106. https://doi.org/10.3390/ijms20051106

Zhang, J., Zhang, S., Li, H., Du, H., Huang, H., Li, Y., Hu, Y., Liu, H., Liu, Y., Yu, G., & Huang, Y. (2016). Identification of transcription factors ZmMYB111 and ZmMYB148 involved in phenylpropanoid metabolism. *Frontiers in Plant Science*, *7*, 148. https://doi.org/10.3389/fpls.2016.00148

Zhao, B., Liu, Q., Wang, B., & Yuan, F. (2021). Roles of phytohormones and their signaling pathways in leaf development and stress responses. *Journal of Agricultural and Food Chemistry*, *69*(12), 3566–3584. https://doi.org/10.1021/acs.jafc.0c07908

Zhao, N., Zhao, X. Q., Zhao, L., Xu, S. X., & Zou, X. Y. (2016). Progress in researches of the response of plant functional traits to grazing disturbance. *Chinese Journal of Ecology*, *35*(7), 1916–1926. https://doi.org/10.13292/j.1000-4890.201607.027

Zhao, Q., & Dixon, R. A. (2011). Transcriptional networks for lignin biosynthesis: More complex than we thought? *Trends in Plant Science*, *16*(4), 227–233. https://doi.org/10.1016/j.tplants.2010.12.005

Zheng, L., Wu, W., Gao, Y., Wu, Y., Xu, Y., Zhang, G., Gao, F., & Zhou, Y. (2022). Integrated transcriptome, small RNA and degradome analysis provide insights into the transcriptional regulatory networks underlying cold acclimation in jojoba. *Scientia Horticulturae*, *299*, 111050. https://doi.org/10.1016/j.scienta.2022.111050

Zheng, S., Lan, Z., Li, W., Shao, R., Shan, Y., Wan, H., Taube, F., & Bai, Y. (2010). Differential responses of plant functional trait to grazing between two contrasting dominant C3 and C4 species in a typical steppe of Inner Mongolia. *Plant and Soil*, *340*(1–2), 141–155. https://doi.org/10.1007/s11104-010-0369-3

Zhu, C., Chen, Y., Li, W., & Ma, X. (2013). Effect of herbivory on the growth and photosynthesis of replanted *Calligonum caput-medusae* saplings in an infertile arid desert. *Plant Ecology*, *215*(2), 155–167. https://doi.org/10.1007/s11258-013-0286-7

Zhu, Y., Qiu, W., He, X., Wu, L., Bi, D., Deng, Z., He, Z., Wu, C., & Zhuo, R. (2022). Integrative analysis of transcriptome and proteome provides insights into adaptation to cadmium stress in *Sedum plumbizincicola*. *Ecotoxicology and Environmental Safety*, *230*, 113149. https://doi.org/10.1016/j.ecoenv.2021.113149

SUPPORTING INFORMATION

Additional supporting information can be found online in the Supporting Information section at the end of this article.

How to cite this article: Liu, Y., Sun, S., Zhang, Y., Song, M., Tian, Y., Lockhart, P. J., Zhang, X., Xu, Y., & Dang, Z. (2024). Integrated transcriptome and proteome analyses reveal potential mechanisms in *Stipa breviflora* underlying adaptation to grazing. *Grassland Research*, 1–17. https://doi.org/10.1002/glr2.12071